Frontiers of Information Technology & Electronic Engineering
www.jzus.zju.edu.cn; engineering.cae.cn; www.springerlink.com
ISSN 2095-9184 (print); ISSN 2095-9230 (online)
E-mail: jzus@zju.edu.cn

Trajectory Poisson multi-Bernoulli filters with unknown detection probability*#

Xiangfei ZHENG, Kaidi LIU, Hongwei LI‡

School of Mathematics and Physics, China University of Geosciences, Wuhan 430074, China

E-mail: zxfdouble@cug.edu.cn; lkd1028@cug.edu.cn; hwli@cug.edu.cn

Received July 18, 2024; Revision accepted Dec. 16, 2024; Crosschecked Oct. 16, 2025; Published online Nov. 27, 2025

Abstract: Compared with general multi-target tracking filters, this paper focuses on multi-target trajectories in scenarios where the detection probability of the sensor is unknown. In this paper, two trajectory Poisson multi-Bernoulli (TPMB) filters with unknown detection probability are proposed: one for alive trajectories and the other for all trajectories. First, an augmented trajectory state with detection probability is constructed, and then two new state transition models and a new measurement model are proposed. Then, this paper derives the recursion of TPMB filters with unknown detection probability. Furthermore, the detailed beta-Gaussian implementations of TPMB filters for alive trajectories and all trajectories are presented. Finally, simulation results demonstrate that the proposed TPMB filters with unknown detection probability can achieve robust tracking performance and effectively estimate multi-target trajectories.

Key words: Trajectory Poisson multi-Bernoulli; Beta-Gaussian; Detection probability; Alive trajectories; All trajectories

https://doi.org/10.1631/FITEE.2400606 **CLC number:** TN391

1 Introduction

Multi-target tracking (MTT) aims to estimate the number of targets of interest in a scene as well as their positions and velocities based on the measurement data containing target position, false alarm and clutter received by sensors (Mahler, 2007, 2014). MTT is widely used in many fields, such as autonomous driving (Chen et al., 2016; Pang et al., 2021), missiles (Menegaz and Battistini, 2018; Yu et al., 2018), robotics (Gao et al., 2020), radar systems (Joshi et al., 2022; Yan et al., 2022), and ship tracking (Granström et al., 2015). For MTT, common solutions include the joint probabilistic data association (JPDA) (Fortmann et al., 1983), multiple hypothesis tracking (MHT) (Blackman, 2004), and random finite set (RFS) framework (Mahler, 2007, 2014). The RFS framework models the target state and the measurement as RFSs, thereby avoiding data association between target states and measurements. Compared with JPDA and MHT, the RFS framework avoids explicit data association and reduces algorithm complexity, thus attracting significant attention from the academic community.

A series of MTT filters based on the RFS framework has been proposed, mainly including the probability hypothesis density (PHD) filter (Vo BN and Ma, 2006), cardinality PHD (CPHD) filter (Vo BT et al., 2007), cardinality balanced multi-target multi-Bernoulli (CBMeMBer) filter (Vo BT et al., 2009), δ-generalized labeled multi-Bernoulli (GLMB) filter (Vo BT and Vo, 2013), and LMB filter (Vo BN

‡ Corresponding author

* Project supported by the National Natural Science Foundation of China (No. 42374174)

Electronic supplementary materials: The online version of this article (https://doi.org/10.1631/FITEE.2400606) contains supplementary materials, which are available to authorized users

ORCID: Xiangfei ZHENG, https://orcid.org/0000-0001-8384-6703; Hongwei LI, https://orcid.org/0000-0001-6809-7097

et al., 2014). The Poisson multi-Bernoulli mixture (PMBM) filter was proposed to solve the problem of undetected targets due to obstruction (García-Fernández et al., 2018; Granström et al., 2020). The PMBM filter is defined as Poisson RFS and multi-Bernoulli mixture (MBM) RFS (García-Fernández et al., 2018) convolution, where Poisson RFS represents undetected targets and MBM RFS represents detected targets. Note that the PMBM filter density is obtained by the MBM filter when the birth model of PMBM is multi-Bernoulli (MB) instead of Poisson. When MB is used to represent detected targets, the PMBM filter density is obtained by the PMB filter (Xia et al., 2022). Similar to GLMB, PMBM is also a multi-target conjugate prior filter. It is important to note that the GLMB filter and LMB filter mentioned above are considered labeled filters, while the others are unlabeled.

Filters can be categorized as either unlabeled, providing an estimate of the target set at the current time, or labeled, providing information about the target set at the current time as well as their trajectories. The GLMB and LMB filters add a unique label to each target state and form a trajectory by associating the target state estimate with the same label. However, the GLMB filter is only suitable for MB birth models and not for independent identically distributed cluster birth models (García-Fernández et al., 2020b).

To estimate the target trajectory, Li TC et al. (2019) proposed the continuous function of time to model the target trajectory, and Houssineau et al. (2021) proposed a multi-target trajectory tracking filter based on possibility theory. In addition to the above trajectory filters, García-Fernández et al. (2020b) proposed an RFS of trajectories (TRFS) that models the trajectory state as a set. TRFS can obtain the target trajectory without using the target label. Then, the TRFS was extended to the PMBM filter, and the trajectory Poisson multi-Bernoulli mixture (TPMBM) filter was proposed by Granström et al. (2018). García-Fernández and Svensson (2019) proposed the trajectory PHD (TPHD) and trajectory CPHD (TCPHD) filters. TCPHD reduces the storage space while maintaining accuracy by adding a track window. When the track window is $L = 1$, TCPHD degrades to CPHD. Gaussian implementations of trajectory Poisson multi-Bernoulli (TPMB) filters for alive trajectories and for all trajectories were provided by García-Fernández et al. (2020c), where the alive trajectories represent trajectories that are still alive in the monitored area at the current time, and all trajectories represent the trajectories that have been presented in the monitoring area. The Gaussian implementation of TPMB filters for alive trajectories estimates the set of alive trajectories at each time step, whereas the other estimates the set of all trajectories at each time step. In these TPMB filters, the Poisson component represents undetected trajectories, and the MB component represents detected trajectories. Due to the true posterior of TPMB being a TPMBM, the TPMB filter is derived by using the Kullback–Leibler divergence (KLD) minimization on a trajectory space with auxiliary variables after each update (García-Fernández et al., 2020c).

It is worth noting that the detection probabilities of all the above filters are given as prior information, and the detection probabilities of sensors are assumed to be constant. However, in real-world scenarios, the detection probability of a sensor is often affected by factors such as its hardware, external environment, and detection distance, resulting in an unknown and time-varying detection probability. To overcome the impact of unknown and time variation detection probability on target tracking, Mahler used a beta distribution to describe the detection probability and proposed the corresponding robust CPHD filter and robust MB filter (Mahler et al., 2011; Vo BT et al., 2013). An unknown detection probability PMBM filter was proposed by Li GC et al. (2021), and robust extended target PMBM filters were further implemented by Wu et al. (2022) and Xie et al. (2023). Although the above filters can achieve multi-target estimation under unknown detection probability, they can only estimate the multi-target state at the current moment and cannot estimate full target trajectories. To directly estimate the trajectory state, Wei et al. (2022) proposed a trajectory RFS filter with unknown detection probability for the first time based on the TCPHD filter. However, the method in Wei et al. (2022) only considers the tracking of alive trajectories within a track window and does not account for tracking all trajectories.

In this paper, TPMB filters with unknown detection probability are proposed to address the issue of tracking alive trajectories and all trajectories. The main contributions are as follows:

1. This paper proposes TPMB filters that can adaptively learn the unknown detection probability while estimating target trajectories. One TPMB filter estimates the set of alive trajectories, while the other estimates the set of all trajectories, with both accounting for unknown detection probability. An augmented trajectory state space model is constructed for the trajectory kinematics and detection probability, and they are propagated by applying the TPMB filters. Moreover, the recursive expressions for the proposed filters are derived.

2. The computationally feasible implementations of the proposed TPMB filters with unknown detection probability are proposed. First, the trajectory state is modeled by the beta-Gaussian (BG) distribution, where the beta distribution is used to model the detection probability and the Gaussian distribution is used to model the kinematic state. Then, closed-form solutions to the TPMB filter for alive trajectories and all trajectories are provided through the BG implementation.

2 Background

This section briefly reviews the TPMB filter. TRFS is expressed in Section 2.1. The TPMBM with auxiliary variable and TPMB approximation filter are reviewed in Sections 2.2 and 2.3, respectively.

2.1 TRFS

Suppose that $x \in \mathbb{R}^{n_x}$ represents the single target state, where n_x denotes the dimension of the state x and x contains the kinematic information of the target, e.g., position and velocity of the target. Then the single trajectory state is represented as $X = \left(t, x^{1:\nu}\right)$, where t represents the initial time of the trajectory, $x^{1:\nu} = \left(x^1, x^2, \ldots, x^\nu\right)$ is a finite sequence of single target states of length ν, and x^i for $i \in \{1, 2, \ldots, \nu\}$ denotes the state of the target at time step $t + i - 1$.

At time step k, for the trajectory $X = \left(t, x^{1:\nu}\right)$, the variable (t, ν) belongs to the set $I_k = \{(t, \nu) : 0 \le t \le k, 1 \le \nu \le k - t + 1\}$, and $X \in T_{(k)} = \uplus_{(t,\nu)\in I_k} \{t\} \times \mathbb{R}^{\nu n_x}$, where $\uplus$ denotes the union of sets that are mutually disjoint and $\times$ denotes a Cartesian product. The set of trajectories up to time k is represented as $X_k = \left\{X_{k,1}, X_{k,2}, \ldots, X_{k,N_{X_k}}\right\} \in \mathcal{F}\left(T_{(k)}\right)$, where $\mathcal{F}\left(T_{(k)}\right)$ is the set of all finite subsets of $T_{(k)}$ and N_{X_k} is the number of elements in the set of trajectories X_k.

2.2 TPMBM with auxiliary variable

In this subsection, the TPMB approximation filter is reviewed. The TPMB approximation filter extends the single trajectory space with an auxiliary variable $u \in \mathbb{U}_k = \{0, 1, \ldots, n_k\}$, such that $\tilde{X} = (u, X) \in \mathbb{U}_k \times T_{(k)}$(García-Fernández et al., 2020c). The variable $u = 0$ denotes an undetected trajectory and corresponds to a Poisson point process (PPP), while the variable $u = i$ denotes a single trajectory corresponding to the i^{th} Bernoulli component. The set of trajectories with an auxiliary variable $\tilde{X}$ belongs to $\mathcal{F}\left(\mathbb{U}_k \times T_{(k)}\right)$. Then the TPMBM with auxiliary variable density at time step k can be represented by

$$\begin{aligned} f_k(\tilde{X}_k) = & \sum_{\left(\uplus_{l=1}^{n_k} \tilde{X}_k^l\right) \uplus \tilde{Y}_k = \tilde{X}_k} f_k^{\mathrm{p}}(\tilde{Y}_k) \\ & \cdot \sum_{a \in \mathcal{A}_k} w_k^a \prod_{i=1}^{n_k} \left[f_k^{i,a^i}\left(\tilde{X}_k^i\right)\right], \end{aligned} \tag{1}$$

where n_k is the number of the Bernoulli component, $\tilde{Y}_k = \left\{(u, X) \in \tilde{X}_k : u = 0\right\}$, and $\tilde{X}_k^i = \left\{(u, X) \in \tilde{X}_k : u = i\right\}$. $f_k^{\mathrm{p}}\left(\tilde{X}\right)$ is the density of Poisson RFS, representing the undetected trajectories as follows:

$$f_k^{\mathrm{p}}(\tilde{X}) = \mathrm{e}^{-\int \lambda_k(\tilde{X})\mathrm{d}\tilde{X}} \left[\lambda_k(\cdot)\right]^{\tilde{X}}, \tag{2}$$

$$\lambda_k(\tilde{X}) = \lambda_k(u, X) = \delta_0[u]\,\lambda_k(X), \tag{3}$$

$$\delta_A[B] = \begin{cases} 1, & A = B, \\ 0, & A \neq B. \end{cases} \tag{4}$$

$f_k^{i,a^i}(\tilde{X})$ is the density of the Bernoulli RFS, representing the detected trajectories as

$$f_k^{i,a^i}(\tilde{X}) = \begin{cases} 1 - r_k^{i,a^i}, & \tilde{X} = \varnothing, \\ r_k^{i,a^i} p_k^{i,a^i}(X)\delta_i[u], & \tilde{X} = \{(u, X)\}, \\ 0, & \text{otherwise}, \end{cases} \tag{5}$$

$$w_k^a = \frac{\prod_{i=1}^{n_k} w_k^{i,a^i}}{\sum_{\theta \in \mathcal{A}_k} \prod_{i=1}^{n_k} w_k^{i,\theta^i}}, \tag{6}$$

where w_k^a denotes the weight of global hypothesis a, with $a = \left(a^1, a^2, \ldots, a^{n_k}\right)$, and $a^i \in \left\{1, 2, \ldots, h^i\right\}$ is the index of the local hypothesis of the i^{th} Bernoulli

component. h^i denotes the number of local hypotheses, w_k^{i,a^i} denotes the weight of local hypothesis a^i related to the i^{th} Bernoulli component, and $\mathcal{A}_k$ is the set of all global hypotheses.

2.3 TPMB approximation

For the TPMBM density with auxiliary variable $f_k(\cdot)$ in Section 2.2, the TPMB approximation density based on minimizing the KLD is defined as follows (García-Fernández et al., 2020c):

$$\tilde{f}_k(\tilde{X}_k) = \tilde{f}_k^{\mathrm{p}}(\tilde{Y}_k) \prod_{i=1}^{n_k} \left[\tilde{f}_k^{i,1}\left(\tilde{X}_k^i\right) \right], \tag{7}$$

where $\tilde{f}_k^{\mathrm{p}}(\tilde{Y}_k)$ is given by Eq. (2) and $\tilde{f}_k^i\left(\tilde{X}_k^i\right)$ is given by Eq. (5) with $a^i = 1$, for $i \in \{1, 2, \ldots, n_k\}$. $a^i = 1$ implies that the i^{th} Bernoulli component retains only one local hypothesis, which is usually omitted from the Bernoulli parameters, i.e., the existence probability and trajectory density in Eq. (5) are r_k^i and $p_k^i(\cdot)$, respectively. Then, the Bernoulli parameters r_k^i and $p_k^i(\cdot)$ are obtained by

$$r_k^i = \sum_{a^i=1}^{h_i} \bar{w}_k^{i,a^i} r_k^{i,a^i}, \tag{8}$$

$$p_k^i(X) = \frac{\sum_{a^i=1}^{h_i} \bar{w}_k^{i,a^i} r_k^{i,a^i} p_k^{i,a^i}(X)}{\sum_{a^i=1}^{h_i} \bar{w}_k^{i,a^i} r_k^{i,a^i}}, \tag{9}$$

where

$$\bar{w}_k^{i,a^i} = \sum_{\theta \in \mathcal{A}_k : \theta^i = a^i} w_k^{\theta}. \tag{10}$$

3 TPMB filters with unknown detection probability

Section 3.1 proposes the augmented trajectory state space model for the set of alive trajectories and the set of all trajectories. The recursions of the TPMB filters with unknown detection probability are provided in Section 3.2.

3.1 Augmented trajectory state space model

Refer to the method in the study of Wei et al. (2022), let $b \in \mathbb{B} = [0, 1]$ denote the single trajectory detection probability space. It is worth noting that b represents the probability that the trajectory itself is detected by the sensor. The variable b is augmented into the single trajectory state to obtain the single augmented trajectory state with an auxiliary variable, such that $\bar{X} = \left(u, \hat{X}\right) \in \mathbb{U}_k \times \hat{\mathbb{X}}_k$, where $\mathbb{U}_k \times \hat{\mathbb{X}}_k$ represents the augmented trajectory state space with an auxiliary variable. $\hat{X} = \left(t, b^{1:\nu}, x^{1:\nu}\right) \in \hat{\mathbb{X}}_k$ denotes the single augmented trajectory state, and the augmented trajectory state space is obtained by

$$\hat{\mathbb{X}}_k = \uplus_{(t,\nu)\in I_k} \{t\} \times \mathbb{B}_k^{\nu} \times \mathbb{R}_k^{\nu n_x}, \tag{11}$$

and $\hat{X}_k \in \mathcal{F}\left(\hat{\mathbb{X}}_k\right)$ denotes the set of augmented trajectories.

To address the TPMB filters with unknown detection probability, we redefine three key components: the state transition model for alive trajectories, the state transition model for all trajectories, and the trajectory measurement likelihood function, all based on the augmented trajectory state space model. In addition, $p^{\mathrm{S}}\left(\bar{X}\right)$ represents trajectory survival probability as shown by García-Fernández et al. (2020c).

1. Transition model of the augmented trajectory state for the set of alive trajectories

At time step k, the single alive trajectory $\hat{X} = \left(t, b^{1:\nu}, x^{1:\nu}\right) \in \hat{X}_k$, where $t + \nu - 1 = k$ and $\hat{X}_k$ is the set of alive trajectories, from time step k to $k+1$, either survives with probability $p^{\mathrm{S}}\left(\hat{X}\right) = p^{\mathrm{S}}(x^{\nu})$ with the transition density

$$\begin{aligned} g_{k+1}\left(t_y, b^{1:\nu_y}, x^{1:\nu_y}|\cdot\right) = & \delta_t\left[t_y\right] \delta_{\nu+1}\left[\nu_y\right] \delta_{x^{1:\nu}}\left[x^{1:\nu_y-1}\right] \\ & \cdot \delta_{b^{1:\nu}}\left[b^{1:\nu_y-1}\right] g_x\left(x^{\nu_y}|x^{\nu}\right) \\ & \cdot g_b\left(b^{\nu_y}|b^{\nu}\right), \end{aligned} \tag{12}$$

or dies with probability $1 - p^{\mathrm{S}}\left(\hat{X}\right)$.

2. Transition model of the augmented trajectory state for the set of all trajectories

At time step k, for the set of all trajectories $\hat{X}_k$, consider a single trajectory $\hat{X} = \left(t, b^{1:\nu}, x^{1:\nu}\right) \in \hat{X}_k$, where $t + \nu - 1 \leq k$. The transition density from time step k to $k+1$ is defined as follows:

$$\begin{aligned} & g_{k+1}\left(t_y, b^{1:\nu_y}, x^{1:\nu_y}|\cdot\right) = \delta_t\left[t_y\right] \\ & \cdot \begin{cases} \delta_{\nu}[\nu_y]\delta_{x^{1:\nu}}[x^{1:\nu_y}]\delta_{b^{1:\nu}}[b^{1:\nu_y}], & \omega_y < k, \\ \delta_{\nu}[\nu_y]\delta_{x^{1:\nu}}[x^{1:\nu_y}] & \\ \cdot\delta_{b^{1:\nu}}[b^{1:\nu_y}]\left(1 - p^{\mathrm{S}}\left(\hat{X}\right)\right), & \omega_y = k, \\ \delta_{\nu+1}[\nu_y]\delta_{x^{1:\nu}}[x^{1:\nu_y-1}]\delta_{b^{1:\nu}}[b^{1:\nu_y-1}] & \\ \cdot p^{\mathrm{S}}\left(\hat{X}\right) g_x\left(x^{\nu_y}|x^{\nu}\right) g_b\left(b^{\nu_y}|b^{\nu}\right), & \omega_y = k+1, \end{cases} \end{aligned} \tag{13}$$

where $\omega_y = t_y + \nu_y - 1$, and $p^{\mathrm{S}}\left(\hat{X}\right) = 1$.

3. Birth model of the augmented trajectory state

At time step k, the newborn augmented trajectory state is born independently following a PPP with intensity

$$\lambda_k^{\mathrm{born}}\left(t, b^{1:\nu}, x^{1:\nu}\right) = \delta_k[t]\,\delta_1[\nu]\,\lambda_b^{\mathrm{born}}\left(b^{\nu}\right)\lambda_x^{\mathrm{born}}\left(x^{\nu}\right). \tag{14}$$

Remark 1 The birth model of the augmented trajectory state for the set of all trajectories is the same as that for the set of alive trajectories.

4. Measurement model of the augmented trajectory state

The measurement model of the augmented trajectory state can be written in the same manner for sets of all trajectories and sets of alive trajectories in the same manner.

At time step k, a single (alive or all) trajectory $\hat{X} = \left(t, b^{1:\nu}, x^{1:\nu}\right) \in \hat{X}_k$ is either detected with probability

$$p_{\mathrm{D}_k}\left(\hat{X}\right) = \begin{cases} b^{\nu}\delta_{k-t+1}[\nu], & t+\nu-1=k, \\ 0, & \text{otherwise}, \end{cases} \tag{15}$$

and generates a measurement with density

$$\begin{aligned} \phi\left(z_k|\hat{X}\right) &= \phi\left(z_k|t, b^{\nu}, x^{\nu}\right)\delta_{k-t+1}[\nu] \\ &= \phi_x\left(z_k|x^{\nu}\right)\delta_{k-t+1}[\nu], \end{aligned} \tag{16}$$

or undetected with probability $1 - p_{\mathrm{D}k}\left(\hat{X}\right)$.

3.2 Recursion of TPMB filters with unknown detection probability

Given a real-valued function $\pi(\cdot)$ on the single augmented trajectory state space $\hat{\mathbb{X}}_k$, its integral is

$$\int \pi\left(\hat{X}\right)\mathrm{d}\hat{X} = \sum_{(t,\nu)\in I_k}\int\int \pi\left(t, b^{1:\nu}, x^{1:\nu}\right)\mathrm{d}b^{1:\nu}\mathrm{d}x^{1:\nu}. \tag{17}$$

Since the detection probability and the kinematic state are independent, Eq. (17) can be rewritten as

$$\begin{aligned} \int \pi\left(\hat{X}\right)\mathrm{d}\hat{X} = \sum_{(t,\nu)\in I_k}&\int \pi_b\left(t, b^{1:\nu}\right)\mathrm{d}b^{1:\nu} \\ &\cdot\int \pi_x\left(t, x^{1:\nu}\right)\mathrm{d}x^{1:\nu}. \end{aligned} \tag{18}$$

Given a real-valued function $\pi(\cdot)$ on the set of augmented trajectory space $\mathcal{F}\left(\hat{\mathbb{X}}_k\right)$, its integral is

$$\begin{aligned} &\int \pi\left(\hat{X}_k\right)\delta\hat{X}_k \\ &= \sum_{N_{\hat{X}_k}=0}^{\infty}\frac{1}{N_{\hat{X}_k}!}\int \pi\left(\left\{\hat{X}_1, \hat{X}_2, \ldots, \hat{X}_{N_{\hat{X}_k}}\right\}\right)\mathrm{d}\hat{X}_{1:N_{\hat{X}_k}}, \end{aligned} \tag{19}$$

where $\int \pi\left(\hat{X}_k\right)\delta\hat{X}_k$ is the set integral (Mahler, 2007, 2014), and $N_{\hat{X}_k}$ is the number of elements in the set of trajectories $\hat{X}_k$.

The inner product of two given real-valued functions $f(\cdot)$ and $g(\cdot)$ on the single augmented trajectory state space is computed as follows:

$$\langle f, g\rangle = \int f\left(\hat{X}\right)g\left(\hat{X}\right)\mathrm{d}\hat{X}. \tag{20}$$

Based on the above, the recursion of the TPMB filter with unknown detection probability is proposed.

3.2.1 Prediction

Suppose that the parameters of the TPMB density for the augmented trajectory state are λ_{k-1} and $\left\{r_{k-1}^i, p_{k-1}^i\left(\hat{X}\right)\right\}_{i=1}^{n_{k-1}}$ at time step $k-1$. At time step k, the predicted density is a TPMB density with $n_{k|k-1} = n_{k-1}$ and

$$\lambda_{k|k-1}\left(\hat{X}\right) = \lambda_k^{\mathrm{born}}\left(\hat{X}\right) + \left\langle \lambda_{k-1}, g_k(\hat{X}|\cdot)p^{\mathrm{S}}(\cdot)\right\rangle, \tag{21}$$

$$r_{k|k-1}^i = r_{k-1}^i\left\langle p_{k-1}^i\left(\hat{X}\right), p^{\mathrm{S}}\right\rangle, \tag{22}$$

$$p_{k|k-1}^i\left(\hat{X}\right) = \frac{\left\langle p_{k-1}^i\left(\hat{X}\right), g_k\left(\hat{X}|\cdot\right)p^{\mathrm{S}}(\cdot)\right\rangle}{\left\langle p_{k-1}^i\left(\hat{X}\right), p^{\mathrm{S}}\right\rangle}, \tag{23}$$

where $\lambda_k^{\mathrm{born}}$, $g_k(\cdot|\cdot)$, and $p^{\mathrm{S}}(\cdot)$ are chosen depending on the case in Section 3.1 for alive trajectories and all trajectories.

3.2.2 Update

Suppose that the parameters of predicted TPMB density for the augmented trajectory state are $\lambda_{k|k-1}$ and $\left\{r_{k|k-1}^i, p_{k|k-1}^i\right\}_{i=1}^{n_{k|k-1}}$ at time step k and the measurement set $z_k = \left\{z_k^1, z_k^2, \ldots, z_k^m\right\}$. Note that the TPMB density for the augmented trajectory state is updated to the TPMBM density.

The parameters of TPMBM density are obtained as follows:

1. Missed detection for PPP

$$\lambda_k\left(\hat{X}\right)=\left(1-p_{\mathrm{D}k}\left(\hat{X}\right)\right)\lambda_{k|k-1}\left(\hat{X}\right). \tag{24}$$

For each Bernoulli component i, $i\in\left\{1,2,\ldots,n_{k|k-1}\right\}$, there are $h^i=m_k+1$ local hypotheses, and the mapping $\mathcal{M}(i,1+j)=\{j\}$, $j\in\{1,2,\ldots,m_k\}$ denotes the measurement z_k^j in the measurement set z_k corresponding to the local hypothesis $1+j$ of the i^{th} Bernoulli component.

2. Missed detection for the Bernoulli component

$$w_k^{i,1}=1-r_{k|k-1}^i\left\langle p_{k|k-1}^i\left(\hat{X}\right),p_{\mathrm{D}k}\left(\hat{X}\right)\right\rangle, \tag{25}$$

$$r_k^{i,1}=\frac{r_{k|k-1}^i\left\langle p_{k|k-1}^i\left(\hat{X}\right),1-p_{\mathrm{D}k}\left(\hat{X}\right)\right\rangle}{1-r_{k|k-1}^i\left\langle p_{k|k-1}^i\left(\hat{X}\right),p_{\mathrm{D}k}\left(\hat{X}\right)\right\rangle}, \tag{26}$$

$$p_k^{i,1}\left(\hat{X}\right)=\frac{\left(1-p_{\mathrm{D}k}\left(\hat{X}\right)\right)p_{k|k-1}^i\left(\hat{X}\right)}{\left\langle p_{k|k-1}^i\left(\hat{X}\right),1-p_{\mathrm{D}k}\left(\hat{X}\right)\right\rangle}, \tag{27}$$

where the local hypothesis is obtained by $\mathcal{M}(i,1)=\varnothing$.

3. Update for the detected Bernoulli component

$$w_k^{i,1+j}=r_{k|k-1}^i\left\langle p_{k|k-1}^i\left(\hat{X}\right),p_{\mathrm{D}k}\left(\hat{X}\right)\phi\left(z_k^j|\cdot\right)\right\rangle, \tag{28}$$

$$r_k^{i,1+j}=1, \tag{29}$$

$$p_k^{i,1+j}\left(\hat{X}\right)=\frac{p_{k|k-1}^i\left(\hat{X}\right)p_{\mathrm{D}k}\left(\hat{X}\right)\phi\left(z_k^j|\cdot\right)}{\left\langle p_{k|k-1}^i\left(\hat{X}\right),p_{\mathrm{D}k}(\hat{X})\phi\left(z_k^j|\cdot\right)\right\rangle}, \tag{30}$$

where the local hypothesis is obtained by $\mathcal{M}(i,1+j)=\{j\}$.

4. New Bernoulli component for the first time

According to García-Fernández et al. (2020c), each measurement generates a new Bernoulli component. Let the new Bernoulli component be $i=n_{k|k-1}+j$, $j\in\{1,2,\ldots,m_k\}$, which is caused by measurement z_k^j. The number of local hypotheses for the i^{th} Bernoulli component is $h_i=2$, with $\mathcal{M}(i,1)=\varnothing$, $w_k^{i,1}=1$, $r_k^{i,1}=0$, and $\mathcal{M}(i,2)=\{j\}$,

$$w_k^{i,2}=\lambda^{\mathrm{C}}\left(z_k^j\right)+\left\langle\lambda_{k|k-1},p_{\mathrm{D}k}\left(\hat{X}\right)\phi\left(z_k^j|\cdot\right)\right\rangle, \tag{31}$$

$$r_k^{i,2}=\frac{\left\langle\lambda_{k|k-1},p_{\mathrm{D}k}\left(\hat{X}\right)\phi\left(z_k^j|\cdot\right)\right\rangle}{\lambda^{\mathrm{C}}\left(z_k^j\right)+\left\langle\lambda_{k|k-1},p_{\mathrm{D}k}\left(\hat{X}\right)\phi\left(z_k^j|\cdot\right)\right\rangle}, \tag{32}$$

$$p_k^{i,2}\left(\hat{X}\right)=\frac{\lambda_{k|k-1}p_{\mathrm{D}k}\left(\hat{X}\right)\phi\left(z_k^j|\cdot\right)}{\left\langle\lambda_{k|k-1},p_{\mathrm{D}k}\left(\hat{X}\right)\phi\left(z_k^j|\cdot\right)\right\rangle}, \tag{33}$$

where λ^C is the clutter density.

The set of global hypotheses is expressed as follows (García-Fernández et al., 2020c):

$$\begin{aligned}\mathcal{A}_k=&\Bigg\{(a_1,a_2,\ldots,a_{n_k}):a_i\in\mathbb{N}_{h^i},\bigcup_{i=1}^{n_k}\mathcal{M}(i,a_i)=\mathbb{N}_{m_k},\\&\mathcal{M}(i,a_i)\bigcap\mathcal{M}(j,a_j)=0,\ \forall i\neq j\Bigg\},\end{aligned} \tag{34}$$

where $\mathbb{N}_{m_k}=\{1,2,\ldots,m_k\}$, and $n_k=n_{k|k-1}+m_k$.

After the above Bernoulli updates, the TPMB density is updated to the TPMBM density. To ensure a closed form of the recursion, the TPMBM density should be approximated to the TPMB density (García-Fernández et al., 2020c).

4 BG TPMB filters

This section introduces the BG implementation of the TPMB filters with unknown detection probability. It provides the prediction and update steps for both alive and all trajectories. The BG implementation for alive trajectories is obtained in Section 4.1, and the BG implementation for all trajectories is obtained in Section 4.2.

The beta distribution for a single trajectory's detection probability is defined as follows:

$$\mathcal{B}\left(t,b^{1:\nu};\tau,\bar{u},\bar{v}\right)=\begin{cases}\mathcal{B}\left(b^{1:\nu};\tau,\bar{u},\bar{v}\right),\ t=\tau,\nu=l,\\0,\ \text{otherwise},\end{cases} \tag{35}$$

where $\bar{u},\bar{v}\in\mathbb{R}^l$, l is the length of the trajectory, and t is the initial time of the trajectory. The beta distribution is presented as follows:

$$\begin{aligned}\mathcal{B}(b;u,v)&=\frac{b^{u-1}(1-b)^{v-1}}{\int_0^1 b^{u-1}(1-b)^{v-1}\,\mathrm{d}b}\\&=\frac{b^{u-1}(1-b)^{v-1}}{\mathcal{B}(b;u,v)},\end{aligned} \tag{36}$$

where $0\leq b\leq 1$, $u>1$, and $v>1$. The expectation of $\mathcal{B}(b;u,v)$ is $\mu=u/(u+v)$, and the covariance of $\mathcal{B}(b;u,v)$ is $\sigma^2=uv/\left((u+v)^2(u+v+1)\right)$.

The Gaussian distribution for the kinematic state of a single trajectory is expressed as follows:

$$\mathcal{N}\left(t, x^{1:\nu}; \tau, \bar{x}, P\right) = \begin{cases} \mathcal{N}\left(x^{1:\nu}; \tau, \bar{x}, P\right), t = \tau, \nu = l, \\ 0, \text{ otherwise}, \end{cases} \tag{37}$$

where $\bar{x} \in \mathbb{R}^{\ln_x}$ is the mean vector and $P \in \mathbb{R}^{\ln_x \times \ln_x}$ is the covariance matrix.

Thus, the trajectory BG function is obtained as follows:

$$\mathrm{BG}\left(\hat{X}; \tau, \varsigma\right) = \mathcal{B}\left(b^{1:\nu}; \tau, \bar{u}, \bar{v}\right) \mathcal{N}\left(x^{1:\nu}; \tau, \bar{x}, P\right), \tag{38}$$

where $\varsigma = (\bar{u}, \bar{v}, \bar{x}, P)$.

In addition, the following assumptions are made:

1. The survival probability of a single trajectory is $p^{\mathrm{S}}\left(x^{\nu}\right) = p^{\mathrm{S}}$.

2. $g_x\left(\cdot|x^{\nu}\right) = \mathcal{N}\left(\cdot; Fx^{\nu}, P\right)$, and $\phi_x\left(\cdot|x^{\nu}\right) = \mathcal{N}\left(\cdot; Hx^{\nu}, R\right)$.

3. The Poisson intensity of birth at time step k is as follows:

$$\lambda_k^{\mathrm{born}}\left(\hat{X}\right) = \sum_{q=1}^{n_k^{\mathrm{born}}} w_k^{\mathrm{born},q} \mathrm{BG}\Big(\hat{X}; k, \bar{u}_k^{\mathrm{born},q}, \bar{v}_k^{\mathrm{born},q}, \bar{x}_k^{\mathrm{born},q}, P_k^{\mathrm{born},q}\Big), \tag{39}$$

where n_k^{born} is the number of components at time step k, $w_k^{\mathrm{born},q}$ is the weight of the q^{th} component, $t^{\mathrm{born},q} = k$ is the start time, $\bar{u}_k^{\mathrm{born},q}$ and $\bar{v}_k^{\mathrm{born},q}$ are the beta distribution parameters, $\bar{x}_k^{\mathrm{born},q}$ is the mean of a Gaussian distribution, and $P_k^{\mathrm{born},q}$ is the covariance matrix of a Gaussian distribution.

4. The Poisson intensity at time step $k-1$ is as follows:

$$\lambda_{k-1}\left(\hat{X}\right) = \sum_{q=1}^{n_{k-1}^{\mathrm{p}}} w_{k-1}^{\mathrm{p},q} \mathrm{BG}\Big(\hat{X}; t_{k-1}^{\mathrm{p},q}, \bar{u}_{k-1}^{\mathrm{p},q}, \bar{v}_{k-1}^{\mathrm{p},q}, \bar{x}_{k-1}^{\mathrm{p},q}, P_{k-1}^{\mathrm{p},q}\Big), \tag{40}$$

where n_{k-1}^{p} is the number of components, $w_{k-1}^{\mathrm{p},q}$ is the weight of the q^{th} component, $t_{k-1}^{\mathrm{p},q}$ is the start time, $\bar{u}_{k-1}^{\mathrm{p},q}$ and $\bar{v}_{k-1}^{\mathrm{p},q}$ are the beta distribution parameters, $\bar{x}_{k-1}^{\mathrm{p},q}$ is the mean of Gaussian distribution, and $P_{k-1}^{\mathrm{p},q}$ is the covariance matrix of Gaussian distribution.

4.1 BG implementation for alive trajectories

In the BG implementation for alive trajectories, the density of the single alive trajectory of the i^{th} Bernoulli component at time step k-1 is considered as follows:

$$p_{k-1}^{i}\left(\hat{X}\right) = \mathrm{BG}\left(\hat{X}; t^{i}, \bar{u}_{k-1}^{i}, \bar{v}_{k-1}^{i}, \bar{x}_{k-1}^{i}, P_{k-1}^{i}\right), \tag{41}$$

where t^i is the start time, $\bar{u}_{k-1}^{i}$ and $\bar{v}_{k-1}^{i}$ are the beta distribution parameters, $\bar{x}_{k-1}^{i}$ is the mean of Gaussian, and P_{k-1}^{i} is the covariance matrix of Gaussian. $\dim\left(\bar{u}_{k-1}^{i}\right) = \dim\left(\bar{v}_{k-1}^{i}\right) = \dim\left(\bar{x}_{k-1}^{i}\right)/n_x$ is the length of trajectory, where $\dim(\cdot)$ denotes the dimensions of the variables. $t^i + \dim\left(\bar{x}_{k-1}^{i}\right)/n_x - 1 = k$ implies that the trajectory is alive at time step k.

The prediction and update steps for alive trajectories are given by the following propositions.

Proposition 1 Suppose that at time $k-1$, the updated parameters of the TPMB filter are $\left\{\lambda_{k-1}, \left\{r_{k-1}^{i}, p_{k-1}^{i}\left(\hat{X}\right)\right\}_{i=1}^{n_{k-1}}\right\}$, where λ_{k-1} and $p_{k-1}^{i}\left(\hat{X}\right)$ are given in Eqs. (40) and (41). The prediction step of the BG implementation for alive trajectories is divided into two parts, PPP and MB, as follows:

1. PPP

$$\lambda_{k|k-1}\left(\hat{X}\right) = p^{\mathrm{S}} \sum_{q=1}^{n_{k-1}^{\mathrm{p}}} w_{k-1}^{\mathrm{p},q} \mathrm{BG}\left(\hat{X}; t_{k-1}^{\mathrm{p},q}, \bar{u}_{k|k-1}^{\mathrm{p},q}, \bar{v}_{k|k-1}^{\mathrm{p},q}, \bar{x}_{k|k-1}^{\mathrm{p},q}, P_{k|k-1}^{\mathrm{p},q}\right) + \lambda_k^{\mathrm{born}}\left(\hat{X}\right), \tag{42}$$

where $\lambda_k^{\mathrm{born}}\left(\hat{X}\right)$ is given by Eq. (39), and

$$\bar{u}_{k|k-1}^{\mathrm{p},q} = \left[\bar{u}_{k-1}^{\mathrm{p},q}, u_{k|k-1}^{\mathrm{p},q}\right]^{\mathrm{T}}, \tag{43a}$$

$$\bar{v}_{k|k-1}^{\mathrm{p},q} = \left[\bar{v}_{k-1}^{\mathrm{p},q}, v_{k|k-1}^{\mathrm{p},q}\right]^{\mathrm{T}}, \tag{43b}$$

$$\bar{x}_{k|k-1}^{\mathrm{p},q} = \left[\bar{x}_{k-1}^{\mathrm{p},q}, \left(\bar{F}_i \bar{x}_{k|k-1}^{\mathrm{p},q}\right)^{\mathrm{T}}\right]^{\mathrm{T}}, \tag{43c}$$

$$P_{k|k-1}^{\mathrm{p},q} = \begin{bmatrix} P_{k-1}^{\mathrm{p},q}, & P_{k-1}^{\mathrm{p},q}\bar{F}_i^{\mathrm{T}} \\ \bar{F}_i P_{k-1}^{\mathrm{p},q}, & \bar{F}_i P_{k-1}^{\mathrm{p},q}\bar{F}_i^{\mathrm{T}} + Q \end{bmatrix}, \tag{43d}$$

$$\bar{F}_i = [0_{1,l^{\mathrm{p},q}-1}, 1] \otimes F, \tag{43e}$$

$$v_{k|k-1}^{\mathrm{p},q} = \left(\frac{\mu(1-\mu)}{\sigma^2} - 1\right)(1-\mu), \tag{43f}$$

$$u_{k|k-1}^{\mathrm{p},q} = \left(\frac{\mu(1-\mu)}{\sigma^2} - 1\right)\mu, \tag{43g}$$

$$\mu = \frac{u}{u+v}, \tag{43h}$$

$$\sigma^2 = \rho\frac{uv}{(u+v)^2(u+v+1)}, \tag{43i}$$

$$u = [0_{1,l^{\mathrm{p},q}-1}, 1]\,\bar{u}_{k-1}^{\mathrm{p},q}, \tag{43j}$$

$$v = [0_{1,l^{\mathrm{p},q}-1}, 1]\,\bar{v}^{\mathrm{p},q}_{k-1}, \tag{43k}$$

where $\otimes$ denotes the Kronecker product, $l^{\mathrm{p},q} = \dim\left(\bar{x}^{\mathrm{p},q}_{k-1}\right)/n_x$, $0_{m,n}$ is an $m \times n$ zero matrix, and $\rho > 1$ is a constant.

2. MB

$$r^i_{k|k-1} = p^{\mathrm{S}} r^i_{k-1}, \tag{44a}$$

$$p^i_{k|k-1}\left(\hat{X}\right) = \mathrm{BG}\left(\hat{X}; t^i, \bar{u}^i_{k|k-1}, \bar{v}^i_{k|k-1}, \bar{x}^i_{k|k-1}, P^i_{k|k-1}\right), \tag{44b}$$

where $\bar{u}^i_{k|k-1}, \bar{v}^i_{k|k-1}, \bar{x}^i_{k|k-1}$, and $P^i_{k|k-1}$ are calculated by replacing $\bar{u}^{\mathrm{p},q}_{k-1}$, $\bar{v}^{\mathrm{p},q}_{k-1}$, $\bar{x}^{\mathrm{p},q}_{k-1}$, and $P^{\mathrm{p},q}_{k-1}$ of Eq. (43) with $\bar{u}^i_{k-1}, \bar{v}^i_{k-1}, \bar{x}^i_{k-1}$, and P^i_{k-1}, respectively.

Proof The proof of Proposition 1 is provided in the supplementary materials.

Proposition 2 Suppose that at time k, the predicted parameters of TPMB are $\left\{\lambda_{k|k-1}, \left\{r^i_{k|k-1}, p^i_{k|k-1}\right\}_{i=1}^{n_{k|k-1}}\right\}$, where $r^i_{k|k-1}$ and $p^i_{k|k-1}$ are obtained in Eqs. (44a) and (44b), $n_{k|k-1} = n_{k-1}$, and $\lambda_{k|k-1}$ are obtained by Eq. (42), and $\lambda_{k|k-1}$ is rewritten as

$$\lambda_{k|k-1}\left(\hat{X}\right) = \sum_{q=1}^{n^{\mathrm{p}}_{k|k-1}} w^{\mathrm{p},q}_{k|k-1}\mathrm{BG}\left(\hat{X}; t^{\mathrm{p},q}_{k-1}, \bar{u}^{\mathrm{p},q}_{k|k-1}, \bar{v}^{\mathrm{p},q}_{k|k-1}, \bar{x}^{\mathrm{p},q}_{k|k-1}, P^{\mathrm{p},q}_{k|k-1}\right), \tag{45}$$

where $n^{\mathrm{p}}_{k|k-1} = n^{\mathrm{p}}_{k-1} + n^{\mathrm{born}}_k$.

The update density can be derived from four cases, which are obtained as follows:

1. Missed detection for PPP

$$\lambda_k\left(\hat{X}\right) = \sum_{q=1}^{n^{\mathrm{p}}_k} w^{\mathrm{p},q}_k \mathrm{BG}\left(\hat{X}; t^{\mathrm{p},q}_k, \bar{u}^{\mathrm{p},q}_k, \bar{v}^{\mathrm{p},q}_k, \bar{x}^{\mathrm{p},q}_k, P^{\mathrm{p},q}_k\right), \tag{46}$$

where

$$w^{\mathrm{p},q}_k = w^{\mathrm{p},q}_{k|k-1}\frac{v^{\mathrm{p},q}}{u^{\mathrm{p},q}+v^{\mathrm{p},q}}, \tag{47a}$$

$$t^{\mathrm{p},q}_k = t^{\mathrm{p},q}_{k-1}, \tag{47b}$$

$$\bar{u}^{\mathrm{p},q}_k = \bar{u}^{\mathrm{p},q}_{k|k-1}, \tag{47c}$$

$$\bar{v}^{\mathrm{p},q}_k = [1_{1,l^{\mathrm{p},q}-1}, 0]^{\mathrm{T}} \odot \bar{v}^{\mathrm{p},q}_{k|k-1} + [0_{1,l^{\mathrm{p},q}-1}, 1]^{\mathrm{T}}\left(v^{\mathrm{p},q}+1\right), \tag{47d}$$

$$\bar{x}^{\mathrm{p},q}_k = \bar{x}^{\mathrm{p},q}_{k|k-1}, \tag{47e}$$

$$P^{\mathrm{p},q}_k = P^{\mathrm{p},q}_{k|k-1}, \tag{47f}$$

where $l^{\mathrm{p},q} = \dim\left(\bar{u}^{\mathrm{p},q}_{k|k-1}\right)$. $u^{\mathrm{p},q}$ and $v^{\mathrm{p},q}$ are obtained by Eqs. (43j) and (43k) using $\bar{u}^{\mathrm{p},q}_{k|k-1}$ and $\bar{v}^{\mathrm{p},q}_{k|k-1}$ instead of $\bar{u}^{\mathrm{p},q}_{k-1}$ and $\bar{v}^{\mathrm{p},q}_{k-1}$, respectively. Here, $A \odot B$ represents the matrix dot product, that is, the multiplication of the corresponding elements of the matrices A and B.

2. Missed detection for the Bernoulli component

$$w^{i,1}_k = 1 - r^i_{k|k-1}\frac{u^i}{u^i+v^i}, \tag{48a}$$

$$r^{i,1}_k = \frac{r^i_{k|k-1}\frac{v^i}{u^i+v^i}}{1 - r^i_{k|k-1}\frac{u^i}{u^i+v^i}}, \tag{48b}$$

$$p^{i,1}_k\left(\hat{X}\right) = \mathrm{BG}\left(\hat{X}; t^i, \bar{u}^{i,1}_k, \bar{v}^{i,1}_k, \bar{x}^{i,1}_k, P^{i,1}_k\right), \tag{48c}$$

where

$$\bar{u}^{i,1}_k = \bar{u}^i_{k|k-1}, \tag{49a}$$

$$\bar{v}^{i,1}_k = [1_{1,l^i-1}, 0]^{\mathrm{T}} \odot \bar{v}^i_{k|k-1} + [0_{1,l^i-1}, 1]^{\mathrm{T}}\left(v^i+1\right), \tag{49b}$$

$$\bar{x}^{i,1}_k = \bar{x}^i_{k|k-1}, \tag{49c}$$

$$P^{i,1}_k = P^i_{k|k-1}, \tag{49d}$$

where $l^i = \dim\left(\bar{u}^i_{k|k-1}\right)$. u^i and v^i are obtained by Eqs. (43j) and (43k) using $\bar{u}^i_{k|k-1}$ and $\bar{v}^i_{k|k-1}$ instead of $\bar{u}^{\mathrm{p},q}_{k-1}$ and $\bar{v}^{\mathrm{p},q}_{k-1}$, respectively.

3. Update for the detected Bernoulli component

For the i^{th} Bernoulli component and the j^{th} measurement z^j_k,

$$w^{i,1+j}_k = r^i_{k|k-1}\frac{u^i}{u^i+v^i}\mathcal{N}\left(z^j_k; \bar{z}_i, S_i\right), \tag{50a}$$

$$p^{i,1+j}_k(\hat{X}) = \mathrm{BG}\left(\hat{X}; t^i, \bar{u}^{i,1+j}_k, \bar{v}^{i,1+j}_k, \bar{x}^{i,1+j}_k, P^{i,1+j}_k\right), \tag{50b}$$

$$\bar{u}^{i,1+j}_k = [1_{1,l^i-1}, 0]^{\mathrm{T}} \odot \bar{u}^i_{k|k-1} + [0_{1,l^i-1}, 1]^{\mathrm{T}}\left(u^i+1\right), \tag{50c}$$

$$\bar{v}^{i,1+j}_k = \bar{v}^i_{k|k-1}, \tag{50d}$$

$$\bar{z}_i = \bar{H}_i \bar{x}^i_k, \tag{50e}$$

$$S_i = \bar{H}_i P^i_{k|k-1}\bar{H}^{\mathrm{T}}_i + R, \tag{50f}$$

$$\bar{H}_i = [0_{1,l^i-1}, 1] \otimes H, \tag{50g}$$

$$\bar{x}^{i,1+j}_k = \bar{x}^i_{k|k-1} + P^i_{k|k-1}\bar{H}^{\mathrm{T}}_i S^{-1}_i\left(z^j_k - \bar{z}_i\right), \tag{50h}$$

$$P^{i,1+j}_k = P^i_{k|k-1} - P^i_{k|k-1}\bar{H}^{\mathrm{T}}_i S^{-1}_i \bar{H}_i P^i_{k|k-1}, \tag{50i}$$

where R represents the measurement noise covariance matrix and H denotes the measurement matrix.

4. New Bernoulli component for the first time

For the new Bernoulli component $i = n_{k|k-1} + j$ generated by measurement $z_k^j, j \in \{1, 2, \ldots, m_k\}$. The component is updated from the predicted Poisson density and corresponds to a new trajectory. The BG component with the highest weight is selected, and the parameters of the new Bernoulli component are initialized with $w_k^{i,1} = 1$, $r_k^{i,1} = 0$, and

$$w_k^{i,2} = \lambda^{\mathrm{C}}\left(z_k^j\right) + \sum_{q=1}^{n_{k|k-1}^{\mathrm{p}}} s^q, \tag{51a}$$

$$r_k^{i,2} = \frac{\sum_{q=1}^{n_{k|k-1}^{\mathrm{p}}} s^q}{w_k^{i,2}}, \tag{51b}$$

$$p_k^{i,2}\left(\hat{X}\right) = \mathrm{BG}\left(\hat{X}; t_{k|k-1}^{\mathrm{p},q*}, \bar{u}_k^{i,2}, \bar{v}_k^{i,2}, \bar{x}_k^{i,2}, P_k^{i,2}\right), \tag{51c}$$

where

$$\bar{u}_k^{i,2} = \left[1_{1,l^i-1}, 0\right]^{\mathrm{T}} \odot \bar{u}_{k|k-1}^{\mathrm{p},q*} + \left[0_{1,l^i-1}, 1\right]^{\mathrm{T}} \left(u^{q*} + 1\right), \tag{52a}$$

$$\bar{v}_k^{i,2} = \bar{v}_{k|k-1}^{\mathrm{p},q^*}, \tag{52b}$$

$$\bar{x}_k^{i,2} = \bar{x}_{k|k-1}^{\mathrm{p},q^*} + P_{k|k-1}^{\mathrm{p},q^*} \bar{H}_i^{\mathrm{T}} S_{q^*}^{-1}\left(z_k^j - \bar{z_{q^*}}\right), \tag{52c}$$

$$P_k^{i,2} = P_{k|k-1}^{\mathrm{p},q^*} - P_{k|k-1}^{\mathrm{p},q*} \bar{H}_{q^*}^{\mathrm{T}} S_{q^*}^{-1} \bar{H}_{q^*} P_{k|k-1}^{\mathrm{p},q^*}, \tag{52d}$$

$$\bar{z_{q^*}} = \bar{H}_{q^*} \bar{x}_{k|k-1}^{\mathrm{p},q^*}, \tag{52e}$$

where $q^* = \mathrm{argmax}_q\left(s^q\right), q \in \left\{1, 2, \ldots, n_{k|k-1}^{\mathrm{p}}\right\}$ and s^q is defined as

$$s^q = \frac{u^q}{u^q + v^q} \mathcal{N}\left(z_k^j; \bar{z_q}, S_q\right), \tag{53a}$$

$$\bar{z_q} = \bar{H}_q \bar{x}_{k|k-1}^{\mathrm{p},q}, \tag{53b}$$

$$\bar{H}_q = \left[0_{1,l^{\mathrm{p},q}-1}, 1\right] \otimes H, \tag{53c}$$

$$S_q = \bar{H}_q P_{k|k-1}^{\mathrm{p},q} \bar{H}_q^{\mathrm{T}} + R, \tag{53d}$$

where $l^{\mathrm{p},q} = \dim\left(\bar{u}_{k|k-1}^{\mathrm{p},q}\right)$, u^q, v^q are obtained by Eqs. (43j) and (43k) using $\bar{u}_{k|k-1}^{\mathrm{p},q}$ and $\bar{v}_{k|k-1}^{\mathrm{p},q}$ instead of $\bar{u}_{k-1}^{\mathrm{p},q}$ and $\bar{v}_{k-1}^{\mathrm{p},q}$, respectively.

Proof The proof of Proposition 2 is provided in the supplementary materials.

Remark 2 After the above undating process. the predicted TPMB density is updated to the TPMBM density. Then, the TPMBM density is approximated to a TPMB filter. Considering that the single trajectory density after the measurement update is a BG mixture, this paper adopts the minimization of the KL divergence to approximate it as a BG distribution. Before merging Bernoulli components, the distance between two BG distributions needs to be calculated. However, the purpose of target tracking is to detect and track, not to calculate the detailed detection probability. Therefore, it is necessary to determine the distance between the two Gaussian distributions. The BG mixture is then merged using criteria similar to those for Gaussian mixtures (Bishop, 2006; Mahler, 2007; García-Fernández et al., 2020c).

The results are provided in the supplementary materials.

4.2 BG implementation for all trajectories

In the BG implementation for all trajectories, we focus on all trajectories that have been detected. Suppose the single trajectory density of the i^{th} Bernoulli component at time step $k-1$ is defined as follows:

$$p_{k-1}^i\left(\hat{X}\right) = \sum_{\varphi=t^i}^{k-1} \beta_{k-1}^i(\varphi)\, \mathrm{BG}\Big(\hat{X}; t^i, \bar{u}_{k-1}^i(\varphi), \bar{v}_{k-1}^i(\varphi), \bar{x}_{k-1}^i(\varphi), P_{k-1}^i(\varphi)\Big), \tag{54}$$

where t^i is the start time of the single trajectory, $\beta_{k-1}^i(\varphi)$ denotes the probability that the corresponding single trajectory terminates at time step φ (García-Fernández et al., 2020c), $\bar{u}_{k-1}^i(\varphi) \in \mathbb{R}^l$, $\bar{v}_{k-1}^i(\varphi) \in \mathbb{R}^l$, $\bar{x}_{k-1}^i(\varphi) \in \mathbb{R}^{\ln_x}$, $P_{k-1}^i(\varphi) \in \mathbb{R}^{\ln_x \times \ln_x}$, $l = \varphi - t^i + 1$, and $\sum_{\varphi=t^i}^{k-1} \beta_{k-1}^i(\varphi) = 1$.

The prediction and update steps for all trajectories are obtained by the following propositions.

Proposition 3 Suppose that at time $k-1$, the updated parameters of TPMB are $\left\{\lambda_{k-1}, \left\{r_{k-1}^i, p_{k-1}^i\left(\hat{X}\right)\right\}_{i=1}^{n_{k-1}}\right\}$, where λ_{k-1} and $p_{k-1}^i\left(\hat{X}\right)$ are defined in Eqs. (40) and (54). $\lambda_{k|k-1}$ is obtained by Eq. (42) and $r_{k|k-1}^i = r_{k-1}^i$. The BG parameters of Eq. (54), for $\varphi \in \left\{t^i, \ldots, k-1\right\}$, are $\bar{u}_{k|k-1}^i(\varphi) = \bar{u}_{k-1}^i(\varphi)$, $\bar{v}_{k|k-1}^i(\varphi) = \bar{v}_{k-1}^i(\varphi)$, $\bar{x}_{k|k-1}^i(\varphi) = \bar{x}_{k-1}^i(\varphi)$, and $P_{k|k-1}^i(\varphi) = P_{k-1}^i(\varphi)$. For $\varphi = k$, $\bar{u}_{k|k-1}^i(\varphi), \bar{v}_{k|k-1}^i(\varphi), \bar{x}_{k|k-1}^i(\varphi)$, and $P_{k|k-1}^i(\varphi)$ are obtained from Proposition 1. Then $\beta_{k|k-1}^i(\varphi)$

is presented as

$$\beta_{k|k-1}^{i}(\varphi)=\begin{cases}\beta_{k-1}^{i}(\varphi),\ \varphi\in\{t^{i},t^{i}+1,\\ \qquad\qquad\ldots,k-2\},\\ \left(1-P^{\mathrm{S}}\right)\beta_{k-1}^{i}(\varphi),\ \varphi=k-1,\\ P^{\mathrm{S}}\beta_{k-1}^{i}(k-1),\ \varphi=k.\end{cases}\tag{55}$$

The proof of Proposition 3 is similar to the proof of Proposition 1. Since a detailed proof is provided for Proposition 1, the proof for Proposition 3 is omitted for brevity.

Remark 3 Following García-Fernández et al. (2020c), the single trajectory density and termination probability remain unmodified for a trajectory considered dead ($\varphi\leq k-2$). For a trajectory considered to have died ($\varphi=k-1$), $\beta_{k|k-1}^{i}(\varphi)$ is calculated using $\left(1-P^{\mathrm{S}}\right)$ and $\beta_{k-1}^{i}(\varphi)$, while its BG trajectory parameters are not propagated. For an alive trajectory ($\varphi=k$), the BG trajectory parameters are propagated as in the case of alive trajectories (see Proposition 1), and $\beta_{k|k-1}^{i}(\varphi)$ is calculated using P^{S} and $\beta_{k-1}^{i}(\varphi)$.

Proposition 4 Suppose the predicted density of TPMB, $p_{k|k-1}^{i}$ and $\lambda_{k|k-1}$ are defined in Eqs. (54) and (45). The missed detection of PPP intensity λ_{k} is obtained by Eq. (46). The misdetection hypothesis for the i^{th} Bernoulli component has the following parameters:

$$w_{k}^{i,1}=1-r_{k|k-1}^{i}\beta_{k|k-1}^{i}(k)\,p_{\mathrm{D}k}^{i},\tag{56a}$$

$$r_{k}^{i,1}=\frac{r_{k|k-1}^{i}\beta_{k|k-1}^{i}(k)\,p_{\mathrm{D}k}^{i}}{1-r_{k|k-1}^{i}\beta_{k|k-1}^{i}(k)\,p_{\mathrm{D}k}^{i}},\tag{56b}$$

$$\beta_{k}^{i,1}(\varphi)=\begin{cases}\beta_{k|k-1}^{i}(\varphi),\ \varphi\in\{t^{i},t^{i}+1,\ldots,k-1\},\\ 1-p_{\mathrm{D}k}^{i}\beta_{k|k-1}^{i}(\varphi),\ \varphi=k,\end{cases}\tag{56c}$$

$$p_{\mathrm{D}k}^{i}=\frac{u^{i}(k)}{u^{i}(k)+v^{i}(k)},\tag{56d}$$

$$u^{i}(k)=\left[0_{1,l^{i}-1},1\right]\bar{u}_{k-1}^{i}(k),\tag{56e}$$

$$v^{i}(k)=\left[0_{1,l^{i}-1},1\right]\bar{v}_{k-1}^{i}(k),\tag{56f}$$

where $l^{i}=\dim\left(\bar{u}_{k-1}^{i}(k)\right)$.

The BG parameters of the trajectory density are as follows:

$$\bar{u}_{k}^{i,1}(\varphi)=\bar{u}_{k|k-1}^{i}(\varphi),\tag{57a}$$

$$\bar{x}_{k}^{i,1}(\varphi)=\bar{x}_{k|k-1}^{i}(\varphi),\tag{57b}$$

$$P_{k}^{i,1}(\varphi)=P_{k|k-1}^{i}(\varphi),\tag{57c}$$

$$\bar{v}_{k}^{i,1}(\varphi)=\begin{cases}\bar{v}_{k|k-1}^{i,1}(\varphi),\ \varphi\in\{t^{i},t^{i}+1,\ldots,k-1\},\\ \bar{v}_{k}^{i,1}(\varphi),\ \varphi=k,\end{cases}\tag{57d}$$

where $\varphi\in\{t^{i},\ldots,k\}$, $\bar{v}_{k}^{i,1}(k)$ is obtained by substituting $\bar{v}_{k|k-1}^{i}(k)$ into Eq. (49b).

For the Bernoulli component i and measurement z_{k}^{j},

$$w_{k}^{i,1+j}=r_{k|k-1}^{i}\beta_{k|k-1}^{i}(k)\,p_{\mathrm{D}k}^{i}\mathcal{N}\left(z_{k}^{j};\bar{z}_{i},S_{i}\right),\tag{58a}$$

$$r_{k}^{i,1+j}=1,\tag{58b}$$

$$\beta_{k}^{i,1+j}(\varphi)=\begin{cases}0, & \varphi\in\{t^{i},t^{i}+1,\ldots,k-1\},\\ 1, & \varphi=k,\end{cases}\tag{58c}$$

$$p_{k}^{i,1+j}\left(\hat{X}\right)=\mathrm{BG}\left(\hat{X};t^{i},\ \bar{u}_{k}^{i,1+j},\bar{v}_{k}^{i,1+j},\bar{x}_{k}^{i,1+j},P_{k}^{i,1+j}\right),\tag{58d}$$

where $\bar{z}_{i}$, S_{i}, $\bar{u}_{k}^{i,1+j}$, $\bar{v}_{k}^{i,1+j}$, $\bar{x}_{k}^{i,1+j}$, and $P_{k}^{i,1+j}$ are given by substituting $\bar{u}_{k|k-1}^{i}(k)$, $\bar{v}_{k|k-1}^{i}(k)$, $\bar{x}_{k|k-1}^{i}(k)$, and $P_{k|k-1}^{i}(k)$ into Eqs. (50c)–(50d) and Eqs. (50h)–(50i), and $p_{\mathrm{D}k}^{i}$ is given by Eq. (56d). The new Bernoulli component $i\in\{n_{k|k-1}+j\}$ is the same as the new Bernoulli component in the TPMB for the alive trajectories described above, but only the Poisson intensity of the alive trajectories is considered in this section. Then, for the new Bernoulli component i, $\beta_{k}^{i,2}(\varphi)$ is set to $\beta_{k}^{i,2}(k)=1$ and $\beta_{k}^{i,2}(\varphi)=0$ for all $\varphi\neq k$.

In addition, the Bernoulli merge for all trajectories is the same as for alive trajectories, obtained by

$$\beta_{k}^{i}(\varphi)=\sum_{a^{i}=1:r_{k}^{i,a^{i}}>0}^{h_{i}}\left[\frac{\bar{w}_{k}^{i,a^{i}}r_{k}^{i,a^{i}}}{r_{k}^{i,}}\beta_{k}^{i,a^{i}}(\varphi)\right],\quad l\in\{t^{i},t^{i}+1,\ldots,k\}.\tag{59}$$

For $\varphi=k$, the proof of Proposition 4 is the same as that of Proposition 2, and for $\varphi\neq k$, the trajectory state is not updated. Therefore, the proof of Proposition 4 is omitted in this paper.

4.3 Estimation

According to García-Fernández et al. (2020c), the trajectory estimation of the updated posterior in Proposition 2 for alive trajectories at time step k is $\left\{\left(t^{i},\bar{b}^{i},\bar{x}^{i}\right):r_{k}^{i}>\Gamma_{d}\right\}$. This set denotes the starting

times, the mean of beta, and the mean of the Gaussian distributions of Bernoulli components whose r_k^i is satisfied with $r_k^i > \Gamma_d$. The mean of beta is estimated as follows:

$$\bar{b}_k^i = \frac{\bar{u}_k^i}{\bar{u}_k^i + \bar{v}_k^i}. \tag{60}$$

For the trajectory estimation of the updated posterior in Proposition 4 for all trajectories at time step k is $\left\{\left(t^i, \bar{b}^i\left(l^*\right), \bar{x}^i\left(l^*\right)\right) : r_k^i > \Gamma_d, l^* = \arg\max_l \beta_k^i\left(l\right)\right\}$. This set denotes the starting times, the mean of beta, and the mean of the Gaussian distributions of Bernoulli components with existence probability greater than Γ_d. $\bar{b}^i\left(l^*\right)$ is obtained by substituting $\bar{u}^i\left(l^*\right)$ and $\bar{v}^i\left(l^*\right)$ into Eq. (61). This paper assumes that all locus source observations are generated at the same time according to the same detection probability. Then, the final output of the detection probability estimation can be averaged over all selected Bernoulli components. Thus, the detection probability is estimated as follows:

$$\hat{b}_k = \frac{1}{\bar{N}_k} \sum_{i=1}^{\bar{N}_k} \bar{b}_k^i, \tag{61}$$

where $\bar{N}_k$ is the number of estimated trajectories, that is, the number of Bernoulli components whose existence probability is greater than Γ_d.

Finally, since TPMB filters with unknown detection probabilities use the same filter recursion for live and all trajectories, Algorithm 1 is used to display the pseudocode for TPMB filters with unknown detection probability.

Algorithm 1 Pseudocode for TPMB filters with unknown detection probability

Input: $\lambda_{k-1}^{\mathrm{u}}$, r_{k-1}^i, $p_{k-1}^i\left(\hat{X}\right)$, n_{k-1}, and z_k
Prediction:
For alive trajectories: apply Proposition 1.
For all trajectories: apply Proposition 3.
Update:
For alive trajectories: apply Proposition 2.
For all trajectories: apply Proposition 4.
Merge the Bernoulli components:
for $i = 1$ to n_k **do**
Compute r_k^{i,a^i} and $\bar{w}_k^{i,a^i}$ using Eqs. (8)–(10).
For alive trajectories: compute $\bar{u}_k^i$, $\bar{v}_k^i$, $\bar{x}_k^i$, and P^i using Eqs. (S14)–(S21).
For all trajectories: compute $\beta_k^i\left(k\right)$, $\bar{u}_k^i\left(k\right)$, $\bar{v}_k^i\left(k\right)$, $\bar{x}_k^i\left(k\right)$, and $P_k^i\left(k\right)$ using Eqs. (S22)–(S30).
end for
Output: λ_k^{u}, r_k^i, p_k^i, and n_k

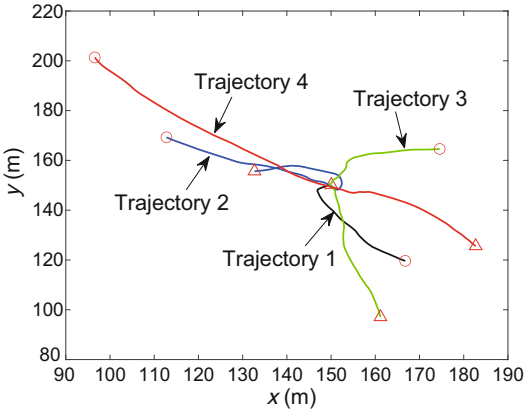

Fig. 1 True trajectories: four truth trajectories are shown in different colors. The circle indicates the starting position of the trajectory, and the triangle indicates the vanishing position of the trajectory. References to color refer to the online version of this figure

5 Simulation results

This section analyzes the performance of the proposed two BG-TPMB filters based on the scenario used by García-Fernández et al. (2020c) and compares them with the BG-TPHD filter (Wei et al., 2022) and the standard TPMB. In standard TPMB, the detection probability is known and provided as a prior. The scenario considers four targets, whose true trajectories are shown in Fig. 1. The target kinematic state is denoted as $x = [p_x, \dot{p_x}, p_y, \dot{p_y}]$, where $[p_x, p_y]^{\mathrm{T}}$ is the two-dimensional position vector and $[\dot{p_x}, \dot{p_y}]$ is the corresponding velocity vector.

Consider the detection probability state $b = [u, v]$. All targets in the scenario follow a nearly constant velocity model, with the kinematic state transition matrix and process noise covariance presented as follows, respectively:

$$F = I_2 \otimes \begin{bmatrix} 1, & T \\ 0, & 1 \end{bmatrix}, Q = qI_2 \otimes \begin{bmatrix} T^3/3, & T^2/2 \\ T^2/2, & T \end{bmatrix}, \tag{62}$$

where I_2 is the identity matrix of order 2, $T = 1$ is the sampling interval, and $q = 0.01$. The trajectory survival probability is set to $p^{\mathrm{S}} = 0.99$. The measurement generator matrix and measurement noise covariance are defined as follows, respectively:

$$H = \begin{bmatrix} 1, & 0, & 0, & 0 \\ 0, & 0, & 1, & 0 \end{bmatrix}, R = \sigma_R^2 I_2, \tag{63}$$

where $\sigma_R^2 = 1$. The number of clutter measurements follows a Poisson distribution with a mean of $\bar{\lambda}_C = 10$, and the clutter is uniformly distributed over the region $[0, 300] \times [0, 300]$.

The Poisson birth intensity for trajectories is a BG mixture with $x_k^{b,1} = [100, 0, 100, 0]^{\mathrm{T}}$, $P_k^{b,1} = \mathrm{diag}([100, 1, 100, 1])$, weight $w_k^{b,1} = 1$ for $k = 1$, and $w_k^{b,1} = 0.005$ for $k \neq 1$. The values of $u_k^{b,1}$ and $v_k^{b,1}$ are discussed in more detail later.

The maximum number of hypotheses of the BG–TPMB filters is set to $N_{\mathrm{h}} = 200$, the pruning thresholds is $\Gamma_{\mathrm{P}} = 10^{-5}$ for PPP weight, and $\Gamma_{\mathrm{mb}} = 10^{-5}$ for MB components, with $L = 5$. The performance of the proposed filters is measured by the root mean square (RMS) $d(\cdot)$ for the trajectories set, i.e.

$$d(k) = \sqrt{\frac{1}{N_{\mathrm{mc}} k} \sum_{i=1}^{N_{\mathrm{mc}}} d^2\left(X_k, \bar{X}_k^i\right)}, \tag{64}$$

where $d(\cdot, \cdot)$ is the linear programming metric with $p = 2, c = 10$, and $\gamma = 1$. N_{mc} is the number of Monte Carlo runs, k indicates the time step, X is the truth set of trajectories, and $\bar{X}$ is the estimation of X (García-Fernández et al., 2020a).

5.1 Scenario 1

To verify the influence of initial beta parameters on the TPMB filters, five different initial beta parameters are set. The initial parameters of the beta distribution are set to $u = [9, 8, 7, 6, 5]$ and $v = [1, 2, 3, 4, 5]$. The detection probability of the sensor is constant at $p_{\mathrm{D}} = 0.9$, the total time step is $N_{\mathrm{s}} = 81$, and $N_{\mathrm{mc}} = 100$.

Fig. 2 shows the detection probability estimations of TPMB for all trajectories under different beta parameters. In Fig. 2, "Truth" represents the true trajectory detection probability $p_{\mathrm{D}} = 0.9$, "9-1-TPMB" represents the BG-TPMB filter for all trajectories with initial beta parameters $u = 9$ and $v = 1$. It can be seen from Fig. 2 that the proposed filter effectively estimates the detection probability. The initial beta parameters are related to the rate at which the sensor's trajectory detection probability converges to the true detection probability. The closer the initial beta parameters are to the detection probability of the sensor, the faster the detection probability converges to the true probability of the sensor.

Fig. 3 shows the trajectory metric error of the

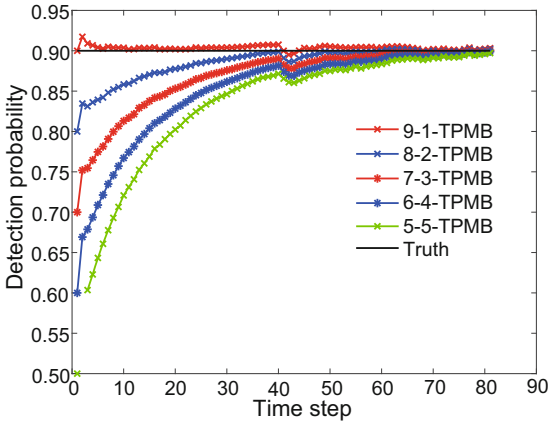

Fig. 2 Estimation of detection probability for all trajectories under different beta parameters

TPMB filter for all trajectories under different initial beta parameters. "Standard-TPMB" represents the TPMB filter that gives the detection probability as prior information. Fig. 4 presents the decomposition of the trajectory metric error. From Figs. 3 and 4, during the first 41 time steps, the trajectory error is inversely correlated with the initial detection probability and the initial parameters of the beta distribution; that is, the initial detection probability is approximately close to the true detection probability, and the error is smaller. After the time step 41, the error is positively correlated with the initial detection probability. In addition, when the trajectory disappears, the error increases. This is due to the slow iteration of beta parameters, which leads to a delay in determining the trajectory's disappearance.

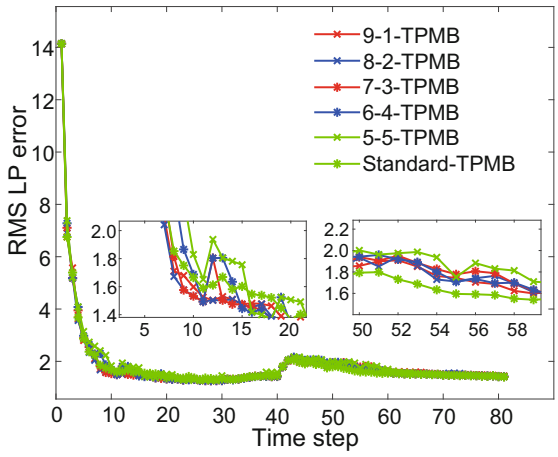

Fig. 3 Trajectory metric errors for all trajectories

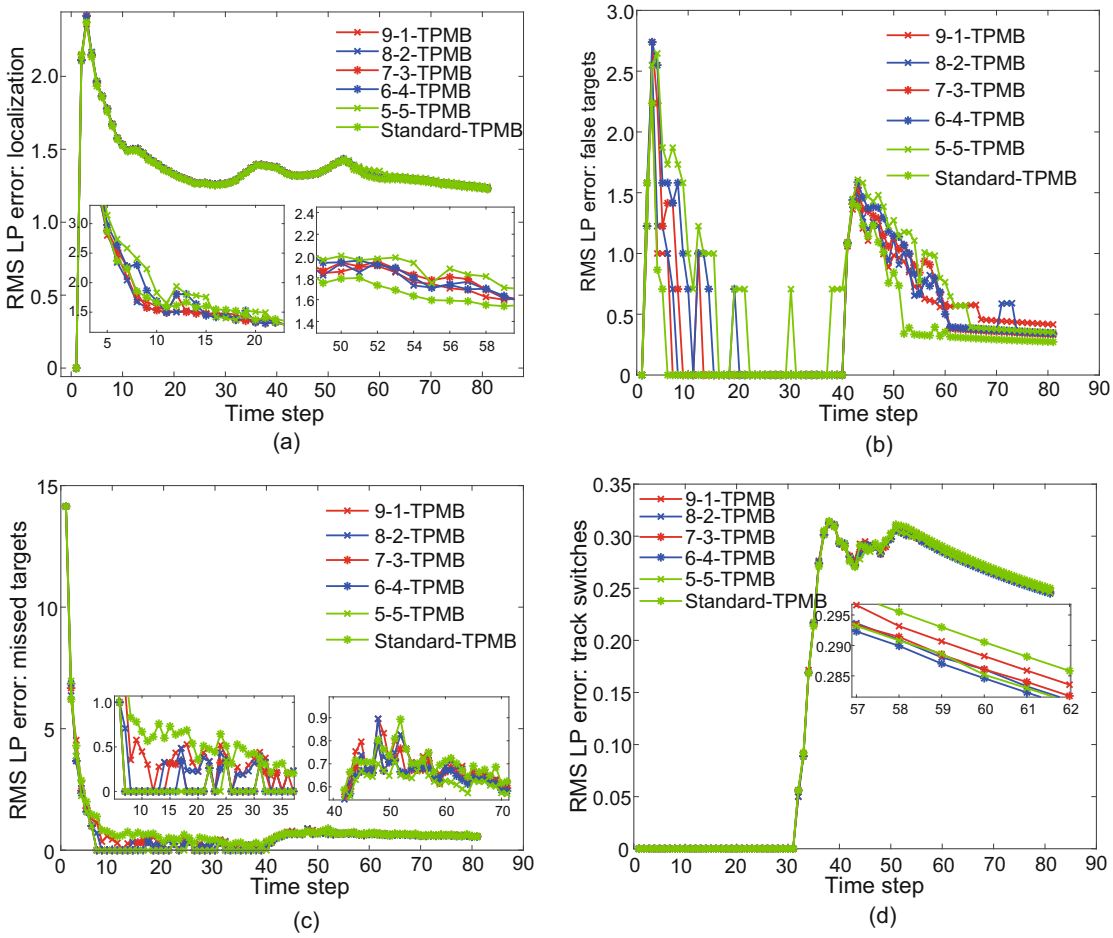

Fig. 4 Decomposition of trajectory metric errors for all trajectories: (a) local error; (b) false error; (c) miss error; (d) switch error

The performance of the proposed filter is further analyzed by setting different clutter rates and detection probabilities. The detection probabilities are set to $p_{\mathrm{D}} = 0.9$ and 0.85, respectively. The closer the initial beta parameter is to the true value of the detection probability, the smaller the error. Therefore, the initial beta distribution parameters are set to $u = 8$ and $v = 2$ for BG-TPMB and BG-TPHD.

Moreover, the clutter rate is set to three different values, $\bar{\lambda}_{\mathrm{C}} = 10$, 20, and 30. The detection probability of standard PMB is set as above. Tables 1 and 2 show the resulting RMS error considering all time steps, calculated as follows:

From Table 1, it can be seen that in the case of unknown sensor detection probability, the performance of the proposed filter is not significantly different from that of the standard TPMB. This indicates that the proposed filter in this paper can effectively estimate the target position when the detection probability is unknown.

As shown in Table 2, as the clutter Poisson rate increases, the errors of all filters increase. With the same detection probability and clutter Poisson rate, the total error of the BG-TPMB algorithm is almost the smallest, while the BG-TPHD filter has the largest error. The overall error of the BG-TPMB filter is smaller than that of the standard TPMB filter. However, in terms of false detection error, the standard TPMB filter outperforms the BG-TPMB filter when p_{D}=0.85.

The average running times of one MC are: 1.18 s (BG-TPMB) and 0.64 s (BG-TPHD). It can be seen that the proposed BG-TPMB filter has better performance than BG-TPHD, but its computational cost is higher. This is always the case with standard

Table 1 Comparison of filter performance under different detection probabilities and clutter rates (all trajectories)

$(p_{\mathrm{D}}, \bar{\lambda}_{\mathrm{C}})$	BG-TPMB					Standard TPMB				
	Total	Local	False	Miss	Switch	Total	Local	False	Miss	Switch
$(0.9, 10)$	2.45	1.40	0.68	1.88	0.21	2.45	1.39	0.56	1.93	0.22
$(0.9, 20)$	2.62	1.41	0.81	2.04	0.22	2.62	1.41	0.73	2.08	0.22
$(0.9, 30)$	2.82	1.45	1.08	2.15	0.21	2.74	1.44	0.81	2.18	0.21
$(0.85, 10)$	2.67	1.46	0.70	2.11	0.22	2.68	1.47	0.64	2.13	0.22
$(0.85, 20)$	2.90	1.51	0.91	2.29	0.21	2.90	1.50	0.84	2.33	0.21
$(0.85, 30)$	3.17	1.51	1.25	2.48	0.22	3.09	1.50	0.97	2.52	0.21

BG: beta-Gaussian; TPMB: trajectory Poisson multi-Bernoulli; Total: total error, calculated from local, false, miss, and switch errors using Eq. (64); Local: local error; False: false error; Switch: switch error

Table 2 Comparison of filter performance under different detection probabilities and clutter rates (alive trajectories)

$(p_{\mathrm{D}}, \bar{\lambda}_{\mathrm{C}})$	BG-TPMB					Standard TPMB					BG-TPHD				
	Total	Local	False	Miss	Switch	Total	Local	False	Miss	Switch	Total	Local	False	Miss	Switch
$(0.9, 10)$	5.43	1.82	3.47	3.74	0.18	5.58	1.84	3.51	3.93	0.18	7.37	1.93	3.78	6.03	0.19
$(0.9, 20)$	5.55	1.85	3.53	3.86	0.18	5.69	1.86	3.57	4.02	0.18	7.61	1.94	3.84	6.28	0.18
$(0.9, 30)$	5.55	1.85	3.56	3.84	0.18	5.69	1.86	3.54	4.04	0.18	7.74	1.95	3.93	6.37	0.19
$(0.85, 10)$	5.54	1.87	3.51	3.85	0.18	5.55	1.88	3.49	3.87	0.18	7.77	1.95	3.78	6.50	0.19
$(0.85, 20)$	5.68	1.91	3.56	3.99	0.17	5.66	1.90	3.51	4.00	0.17	8.07	1.98	3.92	6.77	0.18
$(0.85, 30)$	5.72	1.88	3.61	4.02	0.18	5.73	1.88	3.56	4.07	0.18	8.41	2.04	4.05	7.08	0.18

BG: beta-Gaussian; TPMB: trajectory Poisson multi-Bernoulli; Total: total error, calculated from local, false, miss, and switch errors using Eq. (64); Local: local error; False: false error; Switch: switch error

TPMB and standard TPHD.

$$d_{\mathrm{T}} = \sqrt{\frac{1}{N_{\mathrm{s}}} \sum_{i=1}^{N_{\mathrm{s}}} d^2(k)}.$$

5.2 Scenario 2

In scenario 1, the detection probability is fixed throughout the process, while the sensor tends to reduce the detection probability as the continuous working time becomes longer in actual work. In this section, the detection probability is set as follows:

$$P_{\mathrm{d}}(k) = \begin{cases} 0.9, & k \le 41, \\ 0.8, & k > 41. \end{cases} \tag{65}$$

The initial beta parameters are set to $u = 8, v = 2$. The clutter rate is $\bar{\lambda}_C = 10$. The error of the set for alive trajectories is compared with that of the TPHD filter. The results are shown in Figs. 5–7. The reason for not comparing all trajectories with the TPHD filter is that the TPHD filter does not handle this problem.

Compared to the BG-TPHD filter, the proposed BG-TPMB filter for alive trajectories demonstrates

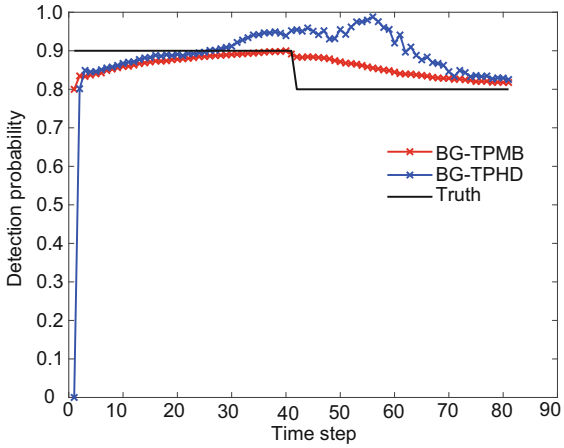

Fig. 5 Estimation of detection probability for alive trajectories

better performance, higher sensitivity to abrupt changes in detection probability, and improved accuracy in estimating detection probability. The trajectory error increases after time step 41, a point where the detection probability and trajectory count change simultaneously. The altered detection probability affects the measurement generation and the

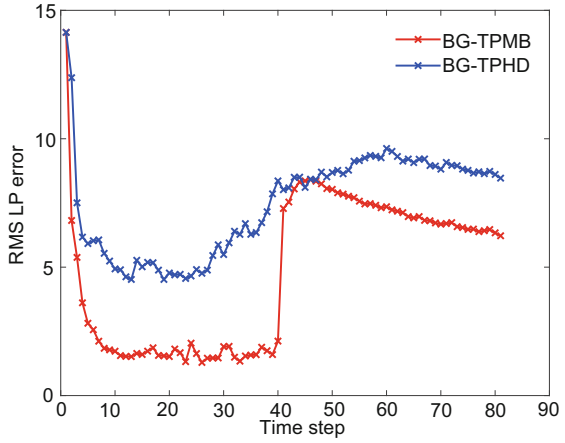

Fig. 6 Trajectory metric error for alive trajectories

clutter profile, which can cause a dead trajectory to be misclassified as alive. Such misclassification, combined with incorrect associations between trajectories and clutter, consequently leads to the observed rise in estimation errors. Additionally, the proposed filter's error rises when a track is lost, which is consistent with the case of the standard TPMB filter for alive trajectories.

The performance of the proposed filter is further analyzed by assigning different detection probabilities to each trajectory. The detection probability of trajectory 1 is 0.95, that of trajectory 2 is 0.9, and that of trajectory 3 and trajectory 4 is 0.8. Moreover, the detection probability of standard TPMB is set to 0.95, and the initial beta parameters are set to $u = 8, v = 2$.

As shown in Fig. 8, the filter proposed in this paper can maintain effective tracking in the face of different detection probabilities for each trajectory. Compared with the standard TPMB, which uses fixed prior-known detection probabilities, the proposed filter achieves better tracking performance.

6 Conclusions

This paper proposes two trajectory TPMB filters that perform robustly when the detection probability is unknown. These filters are implemented

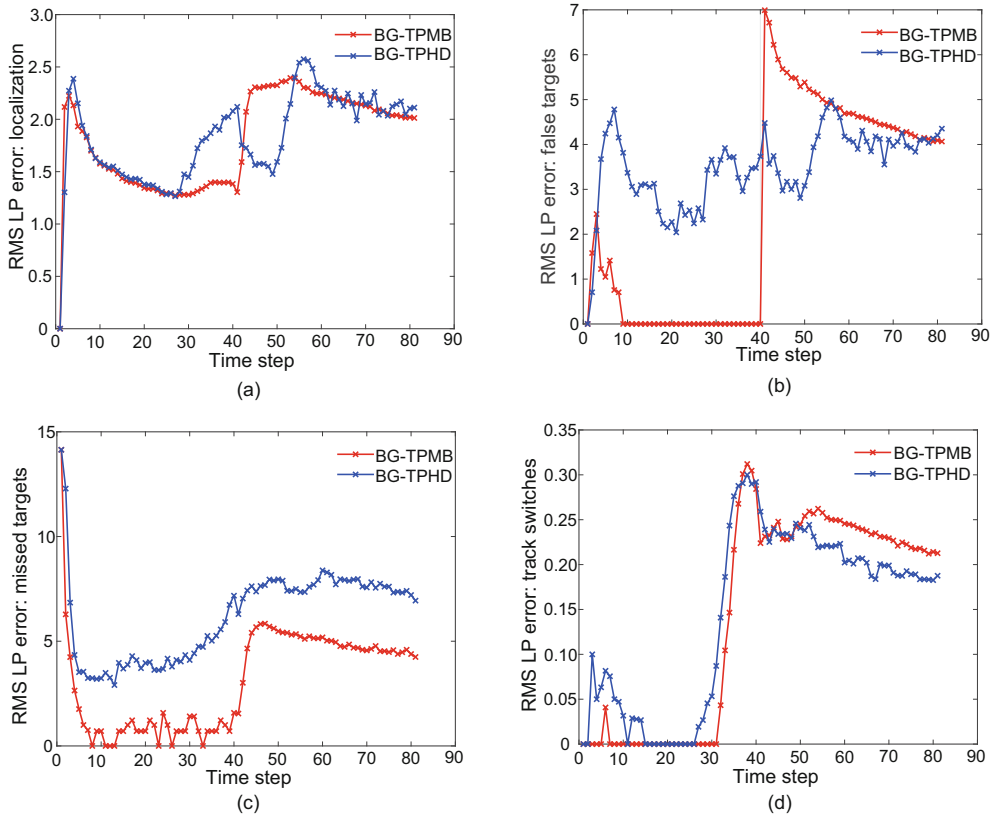

Fig. 7 Decomposition of trajectory metric errors for alive trajectories: (a) local error; (b) false error; (c) miss error; (d) switch error

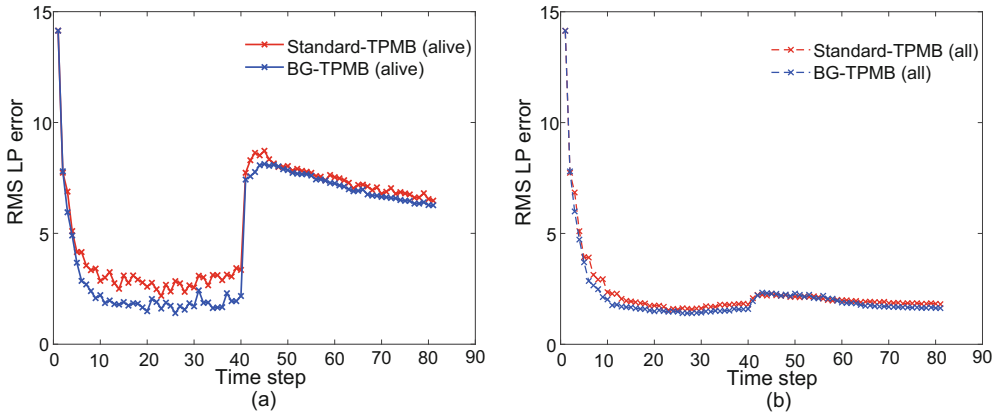

Fig. 8 Trajectory metric error of different detection probabilities for each trajectory: (a) all trajectories error; (b) alive trajectories error

using the BG mixture method, known as BG-TPMB filters. Specifically, the Poisson intensity is approximated as a BG mixture form, and the spatial probability density of each Bernoulli component is approximated as a single BG form. Furthermore, detailed recursive solutions are derived for TPMB filters with unknown detection probability and closed-forms for the BG implementation of alive trajectories and all trajectories are obtained. Finally, simulation results demonstrate that the proposed TPMB filters can adjust to the unknown detection probability and changes in detection over time.

Contributors

Xiangfei ZHENG designed the research. Xiangfei ZHENG and Hongwei LI processed the data. Xiangfei ZHENG drafted the paper. Kaidi LIU and Hongwei LI helped organize the paper. Xiangfei ZHENG, Kaidi LIU, and Hongwei LI revised and finalized the paper.

Conflict of interest

All the authors declare that they have no conflict of interest.

Data availability

The data that support the findings of this study are available from the corresponding author upon reasonable request.

References

Bishop CM, 2006. Pattern Recognition and Machine Learning. Springer, New York, USA.

Blackman SS, 2004. Multiple hypothesis tracking for multiple target tracking. *IEEE Aerosp Electron Syst Mag*, 19(1):5-18. https://doi.org/10.1109/MAES.2004.1263228

Chen TT, Wang RL, Dai B, et al., 2016. Likelihood-field-model-based dynamic vehicle detection and tracking for self-driving. *IEEE Trans Intell Transp Syst*, 17(11):3142-3158. https://doi.org/10.1109/TITS.2016.2542258

Fortmann T, Bar-Shalom Y, Scheffe M, 1983. Sonar tracking of multiple targets using joint probabilistic data association. *IEEE J Oceanic Eng*, 8(3):173-184. https://doi.org/10.1109/JOE.1983.1145560

Gao L, Battistelli G, Chisci L, 2020. Random finite set based distributed multirobot SLAM. *IEEE Trans Robot*, 36(6):1758-1777. https://doi.org/10.1109/TRO.2020.3001664

García-Fernández ÁF, Svensson L, 2019. Trajectory PHD and CPHD filters. *IEEE Trans Signal Process*, 67(22):5702-5714. https://doi.org/10.1109/TSP.2019.2943234

García-Fernández ÁF, Williams JL, Granström K, et al., 2018. Poisson multi-Bernoulli mixture filter: direct derivation and implementation. *IEEE Trans Aerosp Electron Syst*, 54(4):1883-1901. https://doi.org/10.1109/TAES.2018.2805153

García-Fernández ÁF, Rahmathullah AS, Svensson L, 2020a. A metric on the space of finite sets of trajectories for evaluation of multi-target tracking algorithms. *IEEE Trans Signal Process*, 68:3917-3928. https://doi.org/10.1109/TSP.2020.3005309

García-Fernández ÁF, Svensson L, Morelande MR, 2020b. Multiple target tracking based on sets of trajectories. *IEEE Trans Aerosp Electron Syst*, 56(3):1685-1707. https://doi.org/10.1109/TAES.2019.2921210

García-Fernández ÁF, Svensson L, Williams JL, et al., 2020c. Trajectory Poisson multi-Bernoulli filters. *IEEE Trans Signal Process*, 68:4933-4945. https://doi.org/10.1109/TSP.2020.3017046

Granström K, Natale A, Braca P, et al., 2015. Gamma Gaussian inverse Wishart probability hypothesis density for extended target tracking using X-band marine radar data. *IEEE Trans Geosci Remote Sens*, 53(12):6617-6631. https://doi.org/10.1109/TGRS.2015.2444794

Granström K, Svensson L, Xia YX, et al., 2018. Poisson multi-Bernoulli mixture trackers: continuity through random finite sets of trajectories. Proc 21st Int Conf on Information Fusion, p.1-5. https://doi.org/10.23919/ICIF.2018.8455849

Granström K, Fatemi M, Svensson L, 2020. Poisson multi-Bernoulli mixture conjugate prior for multiple extended target filtering. *IEEE Trans Aerosp Electron Syst*, 56(1):208-225. https://doi.org/10.1109/TAES.2019.2920220

Houssineau J, Zeng JJ, Jasra A, 2021. Uncertainty modelling and computational aspects of data association. *Stat Comput*, 31(5):59. https://doi.org/10.1007/s11222-021-10039-1

Joshi SK, Baumgartner SV, Krieger G, 2022. Tracking and track management of extended targets in range-Doppler using range-compressed airborne radar data. *IEEE Trans Geosci Remote Sens*, 60:5102720. https://doi.org/10.1109/TGRS.2021.3084862

Li GC, Kong LJ, Yi W, et al., 2021. Robust Poisson multi-Bernoulli mixture filter with unknown detection probability. *IEEE Trans Veh Technol*, 70(1):886-899. https://doi.org/10.1109/TVT.2020.3047107

Li TC, Chen HM, Sun SD, et al., 2019. Joint smoothing and tracking based on continuous-time target trajectory function fitting. *IEEE Trans Autom Sci Eng*, 16(3):1476-1483. https://doi.org/10.1109/TASE.2018.2882641

Mahler RPS, 2007. Statistical Multisource-Multitarget Information Fusion. Artech House, Boston, USA.

Mahler RPS, 2014. Advances in Statistical Multisource-Multitarget Information Fusion. Artech House, Boston, USA.

Mahler RPS, Vo BT, Vo BN, 2011. CPHD filtering with unknown clutter rate and detection profile. *IEEE Trans Signal Process*, 59(8):3497-3513. https://doi.org/10.1109/TSP.2011.2128316

Menegaz HMT, Battistini S, 2018. Switching multiple model filter for boost-phase missile tracking. *IEEE Trans Aerosp Electron Syst*, 54(5):2547-2553. https://doi.org/10.1109/TAES.2018.2822118

Pang S, Morris D, Radha H, 2021. 3D multi-object tracking using random finite set-based multiple measurement models filtering (RFS-M^3) for autonomous vehicles. Proc IEEE Int Conf on Robotics and Automation, p.13701-13707. https://doi.org/10.1109/ICRA48506.2021.9561852

Vo BN, Ma WK, 2006. The Gaussian mixture probability hypothesis density filter. *IEEE Trans Signal Process*, 54(11):4091-4104. https://doi.org/10.1109/TSP.2006.881190

Vo BN, Vo BT, Phung D, 2014. Labeled random finite sets and the Bayes multi-target tracking filter. *IEEE Trans Signal Process*, 62(24):6554-6567. https://doi.org/10.1109/TSP.2014.2364014

Vo BT, Vo BN, 2013. Labeled random finite sets and multi-object conjugate priors. *IEEE Trans Signal Process*, 61(13):3460-3475. https://doi.org/10.1109/TSP.2013.2259822

Vo BT, Vo BN, Cantoni A, 2007. Analytic implementations of the cardinalized probability hypothesis density filter. *IEEE Trans Signal Process*, 55(7):3553-3567. https://doi.org/10.1109/TSP.2007.894241

Vo BT, Vo BN, Cantoni A, 2009. The cardinality balanced multi-target multi-Bernoulli filter and its implementations. *IEEE Trans Signal Process*, 57(2):409-423. https://doi.org/10.1109/TSP.2008.2007924

Vo BT, Vo BN, Hoseinnezhad R, et al., 2013. Robust multi-Bernoulli filtering. *IEEE J Sel Top Signal Process*, 7(3):399-409. https://doi.org/10.1109/JSTSP.2013.2252325

Wei SX, Zhang BX, Yi W, 2022. Trajectory PHD and CPHD filters with unknown detection profile. *IEEE Trans Veh Technol*, 71(8):8042-8058. https://doi.org/10.1109/TVT.2022.3174055

Wu SY, Zhou YS, Xie Y, et al., 2022. Robust Poisson multi-Bernoulli mixture filter using adaptive birth distributions for extended targets. *Digit Signal Process*, 126:103459. https://doi.org/10.1016/j.dsp.2022.103459

Xia YX, Granström K, Svensson L, et al., 2022. Poisson multi-Bernoulli approximations for multiple extended object filtering. *IEEE Trans Aerosp Electron Syst*, 58(2):890-906. https://doi.org/10.1109/TAES.2021.3111720

Xie XX, Wang Y, Guo JQ, et al., 2023. PMBM filter for multiple extended targets with unknown clutter rate and detection probability. *IEEE Sens J*, 23(15):17133-17147. https://doi.org/10.1109/JSEN.2023.3285885

Yan B, Paolini E, Xu LP, et al., 2022. A target detection and tracking method for multiple radar systems. *IEEE Trans Geosci Remote Sens*, 60:5114721. https://doi.org/10.1109/TGRS.2022.3183388

Yu M, Gong LY, Oh H, et al., 2018. Multiple model ballistic missile tracking with state-dependent transitions and Gaussian particle filtering. *IEEE Trans Aerosp Electron Syst*, 54(3):1066-1081. https://doi.org/10.1109/TAES.2017.2773258

List of supplementary materials

1 Proof of Proposition 1

2 Proof of Proposition 2

3 beta-Gaussian mixture merging